World Journal of Gastrointestinal Oncology

Submit a Manuscript: https://www.f6publishing.com

World J Gastrointest Oncol 2023 June 15; 15(6): 1073-1085

DOI: 10.4251/wjgo.v15.i6.1073

ISSN 1948-5204 (online)

ORIGINAL ARTICLE

Retrospective Study

Relationship between multi-slice computed tomography features and pathological risk stratification assessment in gastric gastrointestinal stromal tumors

Tian-Tian Wang, Wei-Wei Liu, Xian-Hai Liu, Rong-Ji Gao, Chun-Yu Zhu, Qing Wang, Lu-Ping Zhao, Xiao-Ming Fan, Juan Li

Specialty type: Oncology

Provenance and peer review: Unsolicited article; Externally peer reviewed.

Peer-review model: Single blind

Peer-review report's scientific quality classification

Grade A (Excellent): 0
Grade B (Very good): B, B
Grade C (Good): C
Grade D (Fair): 0
Grade E (Poor): 0

P-Reviewer: Huh YM, South Korea; Ojima T, Japan; Terashima M, Japan

Received: March 9, 2023
Peer-review started: March 9, 2023
First decision: March 22, 2023
Revised: April 2, 2023
Accepted: April 25, 2023
Article in press: April 25, 2023
Published online: June 15, 2023

Tian-Tian Wang, Rong-Ji Gao, Chun-Yu Zhu, Xiao-Ming Fan, Juan Li, Department of Medical Imaging, The Second Affiliated Hospital of Shandong First Medical University, Taian 271000, Shandong Province, China

Wei-Wei Liu, Department of Rheumatology, The Second Affiliated Hospital of Shandong First Medical University, Taian 271000, Shandong Province, China

Xian-Hai Liu, Department of Network Information Center, The Second Affiliated Hospital of Shandong First Medical University, Taian 271000, Shandong Province, China

Qing Wang, Department of Ultrasound, The Second Affiliated Hospital of Shandong First Medical University, Taian 271000, Shandong Province, China

Lu-Ping Zhao, Department of Medical Imaging, The Affiliated Hospital of Ji'ning Medical University, Jining 272000, Shandong Province, China

Corresponding author: Juan Li, MM, Attending Doctor, Department of Medical Imaging, The Second Affiliated Hospital of Shandong First Medical University, No. 366 Taishan Street, Taian 271000, Shandong Province, China. 191962554@163.com

Abstract

BACKGROUND

Computed tomography (CT) imaging features are associated with risk stratification of gastric gastrointestinal stromal tumors (GISTs).

AIM

To determine the multi-slice CT imaging features for predicting risk stratification in patients with primary gastric GISTs.

METHODS

The clinicopathological and CT imaging data for 147 patients with histologically confirmed primary gastric GISTs were retrospectively analyzed. All patients had received dynamic contrast-enhanced CT (CECT) followed by surgical resection. According to the modified National Institutes of Health criteria, 147 lesions were classified into the low malignant potential group (very low and low risk; 101

lesions) and high malignant potential group (medium and high-risk; 46 lesions). The association between malignant potential and CT characteristic features (including tumor location, size, growth pattern, contour, ulceration, cystic degeneration or necrosis, calcification within the tumor, lymphadenopathy, enhancement patterns, unenhanced CT and CECT attenuation value, and enhancement degree) was analyzed using univariate analysis. Multivariate logistic regression analysis was performed to identify significant predictors of high malignant potential. The receiver operating curve (ROC) was used to evaluate the predictive value of tumor size and the multinomial logistic regression model for risk classification.

RESULTS

There were 46 patients with high malignant potential and 101 with low-malignant potential gastric GISTs. Univariate analysis showed no significant differences in age, gender, tumor location, calcification, unenhanced CT and CECT attenuation values, and enhancement degree between the two groups ($P > 0.05$). However, a significant difference was observed in tumor size (3.14 ± 0.94 *vs* 6.63 ± 3.26 cm, $P < 0.001$) between the low-grade and high-grade groups. The univariate analysis further revealed that CT imaging features, including tumor contours, lesion growth patterns, ulceration, cystic degeneration or necrosis, lymphadenopathy, and contrast enhancement patterns, were associated with risk stratification ($P < 0.05$). According to binary logistic regression analysis, tumor size [$P < 0.001$; odds ratio (OR) = 26.448; 95% confidence interval (CI): 4.854-144.099)], contours ($P = 0.028$; OR = 7.750; 95%CI: 1.253-47.955), and mixed growth pattern ($P = 0.046$; OR = 4.740; 95%CI: 1.029-21.828) were independent predictors for risk stratification of gastric GISTs. ROC curve analysis for the multinomial logistic regression model and tumor size to differentiate high-malignant potential from low-malignant potential GISTs achieved a maximum area under the curve of 0.919 (95%CI: 0.863-0.975) and 0.940 (95%CI: 0.893-0.986), respectively. The tumor size cutoff value between the low and high malignant potential groups was 4.05 cm, and the sensitivity and specificity were 93.5% and 84.2%, respectively.

CONCLUSION

CT features, including tumor size, growth patterns, and lesion contours, were predictors of malignant potential for primary gastric GISTs.

Key Words: Computed tomography; Gastrointestinal stromal tumor; Risk stratification, Stomach

Core Tip: Gastrointestinal stromal tumors (GISTs) are rare but are nevertheless the most common mesenchymal neoplasms of the gastrointestinal tract. GISTs are most frequently found in the stomach. Preoperative prediction of the malignant potential and prognosis of these GISTs is crucial for clinical decision-making. The present study identified the computed tomography (CT) imaging characteristics for predicting the malignancy risk stratification in 147 patients with primary gastric GISTs. We demonstrated that the qualitative and quantitative features of gastric GISTs on contrast-enhanced CT may be favorable for preoperative risk stratification. This may provide a simple yet effective tool for clinicians to make appropriate clinical decisions.

Citation: Wang TT, Liu WW, Liu XH, Gao RJ, Zhu CY, Wang Q, Zhao LP, Fan XM, Li J. Relationship between multi-slice computed tomography features and pathological risk stratification assessment in gastric gastrointestinal stromal tumors. *World J Gastrointest Oncol* 2023; 15(6): 1073-1085
URL: https://www.wjgnet.com/1948-5204/full/v15/i6/1073.htm
DOI: https://dx.doi.org/10.4251/wjgo.v15.i6.1073

INTRODUCTION

Gastrointestinal stromal tumors (GISTs) are the most common mesenchymal tumors originating in the digestive tract and are thought to be derived from the interstitial cells of Cajal[1,2]. GISTs can arise everywhere in the gastrointestinal tract, but they are predominantly located in the stomach (50%-60%), followed by the small bowel (30%-35%), colon and rectum (5%), and esophagus (< 5%)[3]. They also develop within the mesentery omentum, retroperitoneum, and pelvis. GISTs are classified as borderline tumors, and they range from essentially benign tumors to aggressive sarcomas, and they are physiologically diverse with varied malignant potential[4]. To evaluate the risk of recurrence following complete

resection of primary GISTs, a number of risk categorization techniques have been put forth. The most widely used classification systems for GISTs are the modified National Institutes of Health (NIH) criteria[5] and Armed Forces Institute of Pathology criteria[6], which divide GISTs into four risk categories (very low, low, intermediate, and high risk) based on tumor size, mitotic count, tumor site, and tumor rupture. The 10-year recurrence-free survival rates of patients with the very low-, low-, and intermediate-risk GISTs are 94.9%, 89.7%, and 86.9%, respectively, and are lower in patients with high-risk GISTs (36.2%)[3]. The biological features of GISTs play an essential role in prognosis and evolution, but evaluating their features is usually challenging unless the tumor is excised or has metastasized[7].

The preoperative prediction of the malignant potential and prognosis of these GISTs is crucial for clinical decision-making. Currently, preoperative contrast-enhanced computed tomography (CECT) is regarded as the fundamental imaging modality for the detection and evaluation of GISTs[8,9]. The correlation between CT image features and pathological risk grade of GISTs has been previously reported in some pieces of literature[10-13], revealing that CT imaging features such as tumor location, growth pattern, contour, tumor size, margin, cystic degeneration or necrosis, ulceration, presence of enlarged vessels feeding or draining the mass (EVFDM), contrast enhancement pattern, lymphadenopathy, and direct organ invasion were associated with risk stratification. However, only a few studies have attempted to correlate CT features with the histological grading or prediction of malignancy in the stomach. They have yielded conflicting results because of the limited number of cases[14]. Therefore, the purpose of the present study was to identify the CT imaging characteristics for predicting the malignancy risk stratification in 147 patients with primary gastric GISTs.

MATERIALS AND METHODS

Patients

We enrolled 147 patients with histologically confirmed primary gastric GISTs from the Second Affiliated Hospital of Shandong First Medical University from July 2013 to March 2022. This retrospective study was approved by the Institutional Ethics Committee of the Second Affiliated Hospital of Shandong First Medical University. The inclusion criteria were as follows: (1) Patients underwent curative surgery for primary gastric GISTs; (2) A standard CECT examination was performed within 15 d before surgery; (3) Complete CECT images and clinicopathological data were available; and (4) No distant metastasis at the time of diagnosis. The exclusion criteria were: (1) Patients received treatment before CT and surgery; and (2) Tumor rupture before or during surgery.

Clinical data were reviewed, including age, sex, clinical presentation, and operational styles. There were 74 men and 73 women, aged 31-82 years, with a mean of 61 years. The main symptoms were abdominal pain/discomfort (n = 48), melena (n = 28), and abdominal mass (n = 37). Twenty-five patients were asymptomatic, and the tumors were detected during a regular medical checkup. The remaining nine patients presented with acid reflux, hematemesis, poor appetite and other symptoms. All patients were treated with surgical resection including laparoscopic resection (n = 71), endoscopic resection (n = 46), or open surgery (n = 30). The tumor specimens were subsequently processed for histological examination.

The cases were further categorized according to the risk assessment table published by the modified NIH criteria in 2008[5]. The very low-and low-risk groups were classified into the low malignant potential group, and the intermediate-, high-risk groups were classified into the high malignant potential group. The cohorts were subsequently grouped into the low- and high-grade malignant potential groups.

CT imaging acquisition

All patients underwent abdominal standard CECT before surgery using Philips Brilliance iCT (Philips Medical Systems, Cleveland, OH, United States) and GE LightSpeed VCT (GE Healthcare, Princeton, NJ, United States). Before CT examinations, all patients were fasted for at least 8 h and were encouraged to consume 500-800 mL of water to maximize gastric distension. The scan range covered the upper or entire abdomen, including the pelvic cavity. The acquisition parameters were as follows: Tube voltage, 120 kV; tube current, 300 mAs; slice thickness, 5 mm; slice interval, 5 mm; pitch, 0.9; detector collimation, 64 mm × 0.5 mm; field of view, 350 mm × 350 mm; and matrix, 512 × 512. After the acquisition of unenhanced images, a nonionic iodinated intravenous contrast agent (2.5 mL/kg, 300 mL/mg) was injected intravenously at a rate of 3.0 mL/s. The arterial phase (AP) scan began 25-30 s after injection, while the portal venous phase (PVP) and delayed phase/equilibrium phase scan were started after 55-60 s and 180/120 s, respectively. The original imaging data were reconstructed with a 1.5-mm slice thickness. Axial, sagittal, and coronal multiplanar reconstruction images were obtained with a reconstruction thickness of 2-5 mm. The images were uploaded into the picture archiving and communication system for subsequent analysis.

Imaging analysis

The multi-slice CT scan data were independently reviewed by two radiologists with 13 and 9 years of experience in abdominal imaging, and a consensus was reached for the final interpretations. The pathological diagnosis of GISTs was recorded, but the radiologists were blinded to the pathological data. The CT imaging features were categorized as follows: Tumor size, lesion location (cardia-fundus, body, or antrum), contour (irregular or regular), calcification (presence or absence), cystic degeneration or necrosis (presence or absence), growth patterns (endoluminal, exophytic or mixed), enhancement pattern (heterogeneous or homogenous), degree of contrast enhancement (mild, moderate or marked), and lymphadenopathy (presence or absence). Tumor size was defined as the maximal diameter on the transverse, coronal or sagittal plane. The largest tumor diameter was classified as ≤ 5, 5-10 or > 10 cm. The regular contour was defined as round/ovoid, and irregular was lobulated. Ulceration was considered present when a focal mucosal defect/indentation filled with air or fluid or when contrast material was found on the endoluminal surface of the lesion[13]. Regional lymphadenopathy was considered present if the short-axis diameter of the lymph node was > 1 cm. On CECT scans, areas of cystic degeneration, necrosis, or relative enhancement > 10 HU in any phase were considered heterogeneous enhancement. Necrosis and cystic degeneration were further differentiated. Necrosis was characterized by an irregular low attenuation region without obvious enhancement (≤ 10 HU difference) with a CT attenuation value ≤ 20 HU in each contrast-enhanced phase. Cystic degeneration was characterized by a region with a clear and smooth border and near-water density (CT attenuation value 0-10 HU). The degrees of enhancement for GISTs included absolute and relative enhancement. Absolute enhancement was obtained as the measured CT values in AP, PVP and delayed phase. In contrast, relative enhancement was calculated by the differences in CT values between the unenhanced phase and each enhancement phase. The calculated average values were recorded as the final results. Mild enhancement degree was defined as relative enhancement CT value ≤ 20 HU, and moderate and significant enhancement degrees were 20-40 and > 40 HU, respectively. The CT values of lesions were measured with a 30-50 mm^2 region of interest, selecting the most intensely enhanced solid components of the tumors, excluding tumor vessels, calcification, hemorrhage, and necrotic and cystic regions. The locations of the regions of interest were kept consistent in each phase. Intratumoral necrosis, degree of enhancement, and patterns of enhancement were discerned by PVP CECT scan, and tumor calcification was identified by unenhanced CT.

Statistical analysis

Univariate and multivariate regression analyses were performed with Statistical Package for Social Sciences (SPSS) version 21.0 software packages (SPSS Inc, Chicago, IL, United States), with a two-sided $P < 0.05$ considered statistically significant. Shapiro-Wilk tests were conducted to verify the normality of all variables. Independent samples *t*-tests were conducted for continuous variables (including age, tumor size, attenuation value in noncontrast images, AP and PVP of gastric GISTs with different pathological risk categories. χ^2 tests or Fisher's exact tests were performed to compare the sex and the radiological variables between different risk stratifications (categorical variables). A binary logistic regression analysis was subsequently carried out to identify independent predictors for risk stratification of gastric GISTs. Radiological variables with a $P < 0.05$ in the univariate analysis were enrolled in the binary logistic regression analysis. Odds ratio (OR) with 95% confidence interval (CI) for each risk factor were used to represent the relative risk estimates. Two-sided $P < 0.05$ was considered statistically significant. The statistical chart was created using GraphPad Prism 9 software. The receiver operating curve (ROC) analysis of significant variables was performed, including the CT model from the binary logistic regression analysis. The area under the curve (AUC) was obtained, and the sensitivity, specificity and optimal cutoff values for distinguishing the high-malignant potential from the low-malignant potential group were calculated.

RESULTS

Clinicopathological characteristics of the patients

There were 46 patients with high-malignant potential gastric GISTs (including 27 intermediate grade and 19 high grade), and 101 patients with low-malignant potential gastric GISTs (including 11 very low and 90 low grades). Table 1 displays the characteristics of all the patients involved in this investigation. Age and sex did not significantly differ between the groups with low and high malignant potential, according to a univariate analysis ($P > 0.05$).

CT findings

All 147 patients with gastric GISTs had solitary tumors: 83 (low/high: 55/28) tumors were located in the fundus, 49 (35/14) in the body, and 15 (11/4) in the antrum. In 87 (69/18) patients, the growth patterns of GISTs were endoluminal, in 39 (24/15), exophytic, and in 21 (8/13) individuals, they were mixed types (Figures 1A and 1B).

Table 1 Quantitative features between low-grade and high-grade group

Variables	Low-grade group	High-grade group	χ^2/*Z*/*t* value	*P* value
	n = 101, 68.7%	*n* = 46, 31.3%		
Age (mean ± SD, yr)	60.59 ± 10.33	62.09 ± 11.19	-0.791	0.43
Sex (*n*, %)				
Male	47 (46.5)	26 (56.5)	1.261	0.261
Female	53 (53.5)	20 (43.5)		
Tumor size (mean ± SD), cm	3.14 ± 0.94	6.63 ± 3.26	-9.918	< 0.001
Unenhanced CT, Hu	34.26 ± 3.86	33.93 ± 4.80	0.434	0.665
Absolute enhancement				
AP, Hu	49.72 ± 8.63	47.15 ± 9.44	1.625	0.106
PVP, Hu	60.83 ± 11.07	59.11 ± 11.79	0.858	0.393
DP, Hu	64.68 ± 9.06	63.09 ± 9.12	0.988	0.325
Relative enhancement				
AP, Hu	15.47 ± 7.57	13.22 ± 9.40	1.544	0.125
PVP, Hu	26.57 ± 10.11	25.17 ± 11.69	0.745	0.457
DP, Hu	30.43 ± 7.66	29.15 ± 9.03	0.883	0.379

CT: Computed tomography; AP: Arterial phase; DP: Delayed phase; PVP: Portal venous phase.

The size (largest diameter) of the lesions ranged from 1.0 to 20.7 cm (mean 4.23 cm): 116 (low/high: 98/10) patients had tumor size ≤ 5 cm, and 23 (2/21) had tumor size 5-10 cm, while eight (1/7) had tumor size > 10 cm (Figure 1C). Lesions were irregular in 19 (3/16) patients and regular in 128 (98/30) (Figure 1D). Cystic degeneration or necrosis within lesions was found in 85 (45/40) patients but was absent in 62 (56/6). Ulceration was noted in 48 (25/23) patients but was absent in 99 (76/23). Tumor calcification was found in 22 (14/8) patients but was not seen in 125 (87/38) (Figures 1E and F). Lymphadenopathy was observed in 36 (19/17) patients but was absent in 111 (83/29). On the enhanced CT images, the lesions showed heterogeneous enhancement in 95 (51/44) patients, while homogeneous enhancement was observed in the other 52 (50/2). Primary lesions showed mild enhancement in 12 (6/6) patients, moderate enhancement in 113 (83/30), and marked enhancement in 22 (12/10) on CECT images.

Relationship between CT findings and different risk categories of gastric GISTs (univariate analysis)

Univariate analysis indicated a significant difference in tumor size (3.14 ± 0.94 cm *vs* 6.63 ± 3.26 cm, $P < 0.001$) between the low-grade and high-grade groups. Higher tumor risk was observed with larger tumor size (Figure 2). Tumors with irregular contours were observed more frequently in high-malignant potential GISTs ($P < 0.001$). High-malignant potential GISTs were more likely to exhibit mixed growth, whereas low-malignant potential GISTs predominantly involved endoluminal growth ($P < 0.05$). The presence of ulceration, cystic degeneration or necrosis, lymphadenopathy, and enhancement patterns were significantly different between the two groups ($P < 0.05$). However, there were no appreciable variations between the two groups in terms of any qualitative characteristics, including tumor location, calcification and enhancement degree ($P = 0.760$, 0.578 and 0.075, respectively). There was no significant difference in the risk categories between nonenhancement and each enhancement phase ($P > 0.05$). Table 2 shows the correlation between stomach GIST risk grades and CT findings.

Association of CT features and malignant potential of GISTs (binary logistic regression analysis)

The findings of the univariate analysis revealed that, with the exception of calcification, location, CT values on unenhanced CT and CECT images, and enhancement degree, all of the summary variables in gastric GISTs were linked with risk classes ($P < 0.05$). The CT features that differed significantly in univariate analysis were enrolled in the binary logistic regression analysis. Only tumor size ($P < 0.001$; OR = 26.448; 95%CI: 4.854-144.099), contour ($P = 0.028$; OR = 7.750; 95%CI: 1.253-47.955), and mixed growth ($P = 0.046$; OR = 4.740; 95%CI: 1.029-21.828) were identified as independent predictors for the risk stratification of gastric GISTs (Table 3). The forest plot (Figure 3) included the independent CT characteristics of gastric GISTs with high malignant potential that were obtained using binary logistic regression analysis.

Table 2 Association of computed tomography features and malignant potential in patients with gastric gastrointestinal stromal tumors

Factor	Low risk group (*n* = 101)	High risk group (*n* = 46)	χ^2	*P* value
Location			0.548	0.76
Fundus	55 (54.5)	28 (60.9)		
Body	35 (34.7)	14 (30.4)		
Antrum	11 (10.9)	4 (8.7)		
Tumor diameter (cm)[1]			64.928	< 0.001
> 10 cm	1 (1.0)	7 (15.2)		
5-10 cm	2 (2.0)	21 (45.7)		
≤ 5 cm	98 (97.0)	18 (39.1)		
Tumor contours			28.42	< 0.001
Irregular	3 (3.0)	16 (34.8)		
Regular	98 (97.0)	30 (65.2)		
Ulceration			9.161	0.002
Present	25 (24.8)	23 (50.0)		
Absent	76 (75.2)	23 (50.0)		
Cystic degeneration or necrosis			23.3	< 0.001
Present	45 (44.6)	40 (87.0)		
Absent	56 (55.4)	6 (13.0)		
Calcification			0.309	0.578
Present	14 (13.9)	8 (17.4)		
Absent	87 (86.1)	38 (82.6)		
Growth patterns			14.634	0.001
Mixed	8 (7.9)	13 (28.3)		
Endoluminal	69 (68.3)	18 (39.1)		
Exophytic	24 (23.8)	15 (32.6)		
Lymphadenopathy			5.627	0.018
Present	19 (18.8)	17 (37.0)		
Absent	82 (81.2)	29 (63.0)		
Enhancement pattern			28.192	< 0.001
Heterogeneous	51 (50.5)	44 (95.7)		
Homogenous	50 (49.5)	2 (4.3)		
Enhancement degree			5.188	0.075
Marked	12 (11.9)	10 (21.7)		
Moderate	83 (82.2)	30 (65.2)		
Mild	6 (5.9)	6 (13.0)		

[1]Fisher's exact tests were applied to compare the differences.
χ^2 tests were applied to all other variables.

ROC analysis

ROC analysis for the multinomial logistic regression model and tumor size to differentiate high-malignant potential from low-malignant potential GISTs is shown in Figure 4. The multinomial logistic regression model for gastric GISTs achieved a maximum AUC (0.919; 95%CI: 0.863-0.975), while that for tumor size achieved AUC (0.940; 95%CI: 0.893-0.986). The tumor size cutoff value between the low and high malignant potential groups was 4.05 cm. The sensitivity and specificity were 93.5% and 84.2%,

Table 3 Logistic regression analysis of significant computed tomography features for prediction of high malignant potential

CT feature	β	Odds ratio (95%CI)	*P* value
Size	3.275	26.448 (4.854-144.099)	< 0.001
Contour	2.048	7.750 (1.253-47.955)	0.028
Growth patterns	1.556	4.740 (1.029-21.828)	0.046

CI: Confidence interval; CT: Computed tomography.

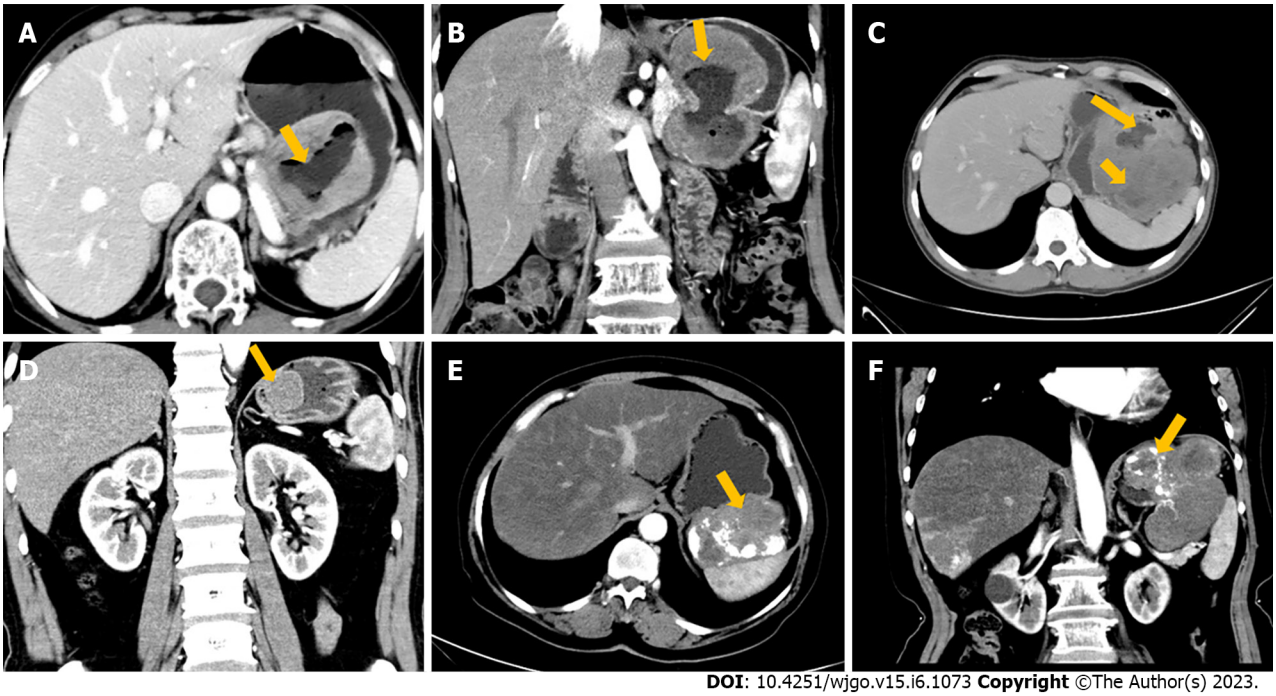

DOI: 10.4251/wjgo.v15.i6.1073 **Copyright** ©The Author(s) 2023.

Figure 1 Computed tomography findings. A and B: A 71-year-old woman with high-risk category gastric gastrointestinal stromal tumor (GIST). Axial (A) and coronal (B) in the arterial phase (AP) computed tomography (CT) images demonstrate an irregular, mixed growth pattern, heterogeneously enhanced tumor with prominent ulceration (arrow); C: A 54-year-old man with high-risk gastric GIST. Axial portal venous phase shows a lesion with a mixed growth pattern, 20-cm, irregular contour, heterogeneous pattern of contrast enhancement with necrotic areas inside (short arrows), and surface ulceration (long arrow); D: A 49-year-old man with low-risk category gastric GIST. Coronal AP shows a 3-cm mass with regular contours, well defined, and homogeneous pattern of contrast enhancement (homogeneous enhancement) (arrow); E and F: A 69-year-old woman with high-risk gastric GIST. Axial (E) and coronal (F) contrast-enhanced CT images in the AP show a lobular, well-defined tumor with exophytic growth pattern and heterogeneous pattern of contrast enhancement, with prominent calcification and necrotic areas inside (arrows).

respectively (Figure 4).

DISCUSSION

GISTs are rare but are nevertheless the most common mesenchymal neoplasms of the gastrointestinal tract. GISTs are most frequently found in the stomach. Numerous investigations have revealed a connection between the anatomical placement and the biological behavior of GISTs[5,6]. Tang *et al*[14] compared the CT features of gastric and small bowel GISTs to evaluate their association with risk grades and showed that small bowel and stomach GISTs had considerably different risk grades. Tumors originating in the stomach are less aggressive than tumors of intestinal origin[14].

For detection, qualitative diagnosis, staging, assessment of therapy response, follow-up after surgery, and forecasting of rupture and biologic aggressiveness, CT is the primary imaging modality[15-17]. The development of risk-segmented GISTs can be predicted using CECT, according to a number of studies [13,18,19], and many of them involved intestinal GISTs[16,20]. However, to our knowledge, only a few studies have focused on the association of gastric GIST CT findings and the degree of malignancy or mitotic rate and metastatic risk. There has been research on the correlation between CT findings and the degree of mitotic rate[20]. As NIH standards 2008 for GISTs risk stratifications are widely accepted, only

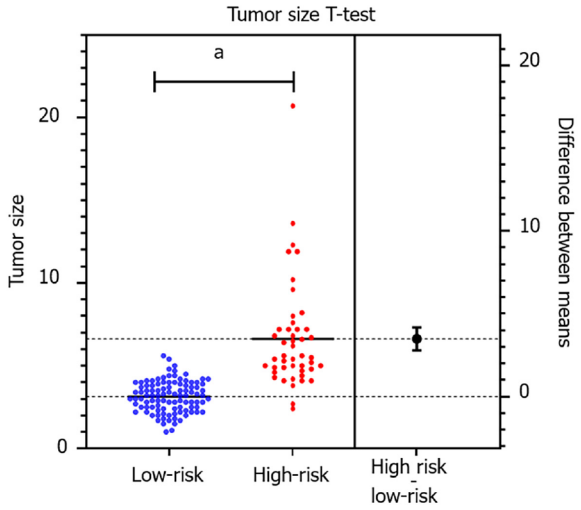

DOI: 10.4251/wjgo.v15.i6.1073 **Copyright** ©The Author(s) 2023.

Figure 2 Independent sample *t*-test estimation chart. [a]*P* < 0.0001.

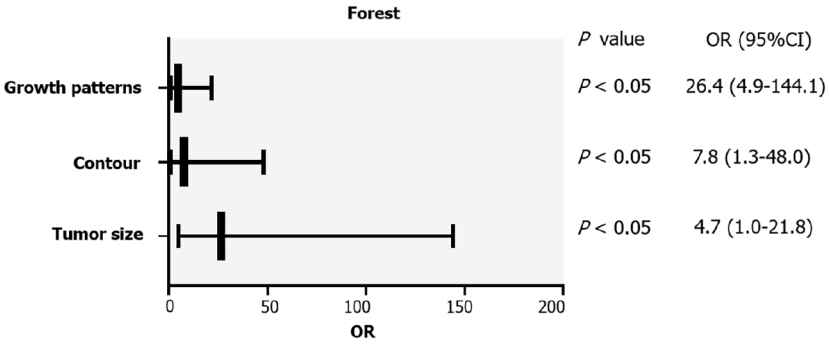

DOI: 10.4251/wjgo.v15.i6.1073 **Copyright** ©The Author(s) 2023.

Figure 3 Forest plot of the independent computed tomography features of gastric gastrointestinal stromal tumor with high malignant potential. OR: Odds ratio; CI: Confidence interval.

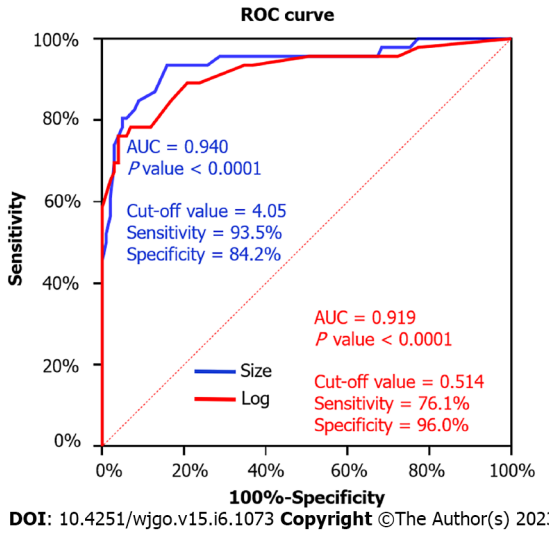

DOI: 10.4251/wjgo.v15.i6.1073 **Copyright** ©The Author(s) 2023.

Figure 4 Receiver operating curve for tumor size and the multinomial logistic regression model to differentiate high-malignant potential from low-malignant potential gastrointestinal stromal tumor. ROC: Receiver operating curve; AUC: Area under the curve.

a few studies[14,21,22] enrolled patients with gastric GIST to evaluate the predictive value of CT imaging features for risk stratification. However, the variation in results may be due to the different inclusion criteria and subjective assessment standards.

Numerous studies have shown that different CT imaging features, including as lesion margin, size, shape, necrosis, ulceration, growth patterns, enhancement pattern, EVFDM, direct organ invasion, and lymphadenopathy, are related to risk classification. However, logistic regression analysis only identified a few CT features of the primary tumor as independent risk stratification predictors.

Li *et al*[10] analyzed the CT features of gastric GISTs, including size, location (cardiac/pericardial region, fundus, body, or antrum), EVFDM, necrosis, ulceration, growth pattern, contour, mesenteric fat infiltration, and direct organ invasion. The results revealed that tumor size, cardia/pericardial origin, EVFDM, and mesenteric fat infiltration might be independent indicators of high malignant potential.

The study by Tang *et al*[14] reported that only tumor size, necrosis and the difference of CT values between AP and PVP were independent factors influencing the risk stratification of gastric GISTs. For small bowel GISTs, the independent predictors were tumor size and ulceration. In the study about GISTs, Zhou *et al*[12] reported that CT imaging features, including tumor margin, size, shape, tumor growth pattern, direct organ invasion, necrosis, EVFDM, lymphadenopathy, and contrast enhancement pattern, were associated with the risk stratifications. However, in multinomial logistic regression analysis, only lesion size, development pattern, and EVFDM were recognized as independent risk factors.

In this study, 147 cases of gastric GISTs were retrospectively analyzed and the CT features such as location, size, contour, necrosis or cystic degeneration, ulceration, growth pattern, lymphadenopathy and contrast enhancement were correlated with the risk and prognosis of malignancy. Both the low-malignant potential group (very low and low risk) and the high-malignant potential group (mid and high risk) were created from the 147 patients. Our research demonstrated that the tumor size, contour, presence of necrosis or cystic generation, ulceration and lymphadenopathy, tumor growth pattern and enhancement pattern were significant factors for risk stratification of GISTs. However, only tumor size (> 5 cm), irregular contours, and mixed growth pattern were independent predictors for high malignant potential in multivariate logistic regression analysis (OR = 26.448, 7.750 and 4.740, respectively). We transformed the above independent factors into the CT model for risk stratification of gastric GISTs. The AUC of the ordinal multinomial logistic regression model was 0.919, which shows that the risk stratifications may be reasonably predicted by the logistic regression model.

Rubin *et al*[23] reported that the risk of developing gastric GISTs was the same for both sexes, and although they occurred over a wide age distribution, about 75% were diagnosed in patients older than 50 years. Univariate analysis revealed that the prognosis of GISTs was independent of age and sex in the present study, and the mean age of the patients was 61 years, which is consistent with our research.

Gastric GISTs can occur anywhere but are more common in the fundus of the stomach. In this study, 56.46% (83/147) of tumors were located in the gastric fundus and 33.33% (49/147) in the gastric body, while the gastric antrum accounted for 10.20% (15/147). However, there was no significant difference between the location of the GISTs in the stomach and the risk stratification of the GISTs.

Tumor size is considered one of the most commonly used and reliable indicators for assessing GIST risk. The multivariate analysis in this study revealed that tumor size was an independent influencing factor for risk stratification of gastric GISTs, with a cut-off value of 4.05 cm. Tumor size is a component of the modified NIH criteria. A larger tumor size tends to suggest a more aggressive biological behavior. These results corroborate many earlier findings[23-25].

In terms of tumor contours, we demonstrated that gastric GISTs with a high-risk malignant potential were more likely to have an irregular tumor shape on CT. Our results are consistent with the study by Iannicelli *et al*[26], which found that irregular contours were the only CT feature that showed a linear correlation with risk. As the risk increases, the likelihood of detecting irregular margins of the gastric GISTs also increases. With higher tumor risk, higher tumor volume, disordered mitotic phase, invasive mesenchyma, and irregular contours are usually observed. Many studies have found that large stromal tumors were irregular and lobulated[27,28]. Wei *et al*[29] investigated the relationship between risk stratification and the shape of GISTs and reported that the method for quantifying tumor shape predicted the risk level and mitotic value of GISTs.

In our study, mixed growth patterns were independent predictors for high malignant potential. Endoluminal growth was detected in 59.18% (87/147) cases, exophytic growth in 26.53% (39/147) cases, and 21 patients showed mixed growth patterns, including 13 in the high-risk potential group, accounting for 61.90%. Our research revealed that compared to primary lesions with an endoluminal development pattern, those with mixed growth patterns were more likely to have greater GIST risk stratification. However, there is inconsistency in the literature on whether different GIST growth patterns are beneficial for judging the risk of GIST[10,12,22]. Therefore, further research is required in the future.

Peng *et al*[22] demonstrated that high-risk gastric GISTs were likely to present with necrosis even though it was not an independent predictor, which is consistent with our study. However, the studies by Liu *et al*[30] and Tang *et al*[14] demonstrated that tumor necrosis was an independent predictor of unfavorable disease-free survival in gastric GISTs. One possible explanation for the discrepancy may be that tumor necrosis is more common in the high-malignant potential group and is sometimes difficult to

be identified with the naked eye. However, these results suggested that tumor necrosis was a significant factor in classifying the malignancy of gastric GISTs. Even though necrosis was not an independent predictor, the research by Peng *et al*[22] showed that high-risk gastric GISTs were likely to present with it, which is consistent with our analysis. Tumor necrosis was found to be an independent predictor of poor disease-free survival in gastric GISTs, according to research by Liu *et al*[30] and Tang *et al*[14]. Tumor necrosis, which can be challenging to detect with the unaided eye sometimes, is more prevalent in the group of patients with high-malignant potential, which may be one reason for the discrepancy. These findings, however, revealed that tumor necrosis had a substantial role in determining the degree of malignancy of gastric GISTs.

The consistency between pathology and CT in identifying tumor necrosis should be validated. In our study, necrosis or cystic lesions and ulcers were also found to be important factors in the risk stratification of GISTs. In contrast, we found no significant difference between calcification and risk category, which was similar to previous studies[13,14].

The heterogeneous pattern of contrast enhancement was mainly observed in high-risk gastric GISTs. In contrast, tumors belonging to the low-risk classes mostly appeared with a homogeneous pattern of contrast enhancement. The result is consistent with the study of Iannicelli *et al*[26]. A high degree of contrast enhancement is usually considered a characteristic of tumor biological activity, but was not associated with the risk stratification in our research, which was in accordance with previous studies[13,26]. However, the enhancement degree plays an important role in distinguishing GISTs from other tumors such as leiomyomas[31].

Hong *et al*[32] reported that lymph node metastases are extremely rare, but a recent study by Zhou *et al*[12] of > 120 patients with histologically confirmed primary GISTs reported that lymphadenopathy was associated with risk stratification. In this study, a significant difference in lymphadenopathy was found between the low malignant potential and high malignant potential groups (18.81% *vs* 36.96%, respectively). We believe that lymphadenopathy around the lesion is more likely to occur in tumors with high malignant potential. However, among the 36 lymph nodes reported, only one had a short diameter > 1 cm. Therefore, the clinical significance of lymphadenopathy should be further studied.

The present investigation included some restrictions. First of all, because it was a retrospective study conducted by just one institution, there may have been selection bias. Secondly, signs such as hemorrhage, EVFDM, tumor margin, peripheral fat infiltration, and other organ invasion were not evaluated.

CONCLUSION

Tumor size, contours and growth pattern were significant independent predictors for identifying high-risk patients, while primary GIST > 5 cm, irregular contours, or mixed growth patterns indicate a potentially high-risk tumor. In addition, tumor necrosis or cystic degeneration, ulceration, enhancement patterns and lymphadenopathy on dynamic CECT could improve the prognostic accuracy of patients with gastric GISTs. As a result, our study showed that preoperative risk stratification may benefit from the qualitative and quantitative characteristics of stomach GISTs on CECT. Clinicians may be given a straightforward yet useful tool to use in order to choose the best surgical method and administer preoperative neoadjuvant therapy.

Future prospective and multicenter studies will be required to confirm our early findings. Magnetic resonance imaging and positron emission tomography combined with CT may predict the malignant potential of gastric GISTs, and dual-energy CT may be used in the assessment. These aspects should be further studied. In addition, artificial intelligence should be applied in future research to assess the prognosis of GISTs.

ARTICLE HIGHLIGHTS

Research background

Clinical decision-making depends on preoperative assessment of the likelihood of malignancy and prognosis of these gastrointestinal stromal tumors (GISTs). Correlation between computed tomography (CT) image features of GIST and pathological risk grade has been previously reported in several publications. However, only a few studies have attempted to correlate CT features with histologic grading or prediction of gastric malignancy.

Research motivation

The research is to explore the multi-slice CT imaging features for predicting risk stratification in patients with primary gastric GISTs, and to give clinicians a straightforward yet useful tool to use in choosing the best surgical approach and preoperative neoadjuvant therapy.

Research objectives
The purpose of this study was to identify the CT imaging characteristics for predicting risk stratifications in patients with primary gastric GISTs.

Research methods
This retrospective analysis of clinicopathological and CT imaging data for 147 patients with gastric GISTs. The association between malignant potential and CT features was analyzed using univariate analysis and multivariate logistic regression analysis, receiver operating curve was used to evaluate the predictive value of tumor size, and the multinomial logistic regression model for risk classification.

Research results
Tumor size, tumor contours, lesion growth patterns, ulceration, cystic degeneration or necrosis, lymphadenopathy, and contrast enhancement patterns, were associated with the risk stratification; tumor size, contours and growth pattern were independent predictors for risk stratification of gastric GISTs.

Research conclusions
CT features, including tumor size, growth patterns, and lesion contours, were predictors of malignant potential for primary gastric GISTs.

Research perspectives
The CT characteristics could offer clinicians a straightforward yet useful tool for making smart clinical judgments.

FOOTNOTES

Author contributions: Wang TT designed and performed the research and wrote the paper; Li J designed the research and supervised the report; Liu XH designed the research and contributed to the analysis; Liu WW, Gao RJ, Zhu CY, and Wang Q provided clinical advice; Zhao LP and Fan XM supervised the report.

Supported by the Roentgen Imaging Research Project of Beijing Kangmeng Charitable Foundation, No. SD-202008-017.

Institutional review board statement: This study was approved by the Institutional Ethics Committee of the Second Affiliated Hospital of Shandong First Medical University (2022-016).

Informed consent statement: This is retrospective study that used anonymous clinical data. According to institutional policies, informed consent was not required from patients in this study.

Conflict-of-interest statement: All the authors report no relevant conflicts of interest for this article.

Data sharing statement: The data for this study can be obtained from the corresponding author upon request.

Country/Territory of origin: China

ORCID number: Tian-Tian Wang 0000-0003-3872-1949; Wei-Wei Liu 0000-0001-8606-5777; Xian-Hai Liu 0000-0001-9706-7196; Rong-Ji Gao 0000-0002-7385-6438; Chun-Yu Zhu 0000-0002-3622-2073; Qing Wang 0000-0001-9430-1442; Lu-Ping Zhao 0000-0002-4945-2820; Xiao-Ming Fan 0000-0002-1555-225X; Juan Li 0000-0003-1254-5748.

S-Editor: Wang JJ
L-Editor: A
P-Editor: Yu HG

REFERENCES

1 **Fletcher CD**, Berman JJ, Corless C, Gorstein F, Lasota J, Longley BJ, Miettinen M, O'Leary TJ, Remotti H, Rubin BP, Shmookler B, Sobin LH, Weiss SW. Diagnosis of gastrointestinal stromal tumors: a consensus approach. *Int J Surg Pathol*

2002; **10**: 81-89 [PMID: 12075401 DOI: 10.1177/106689690201000201]
2 **Cola D**, Bahoura L, Copelan A, Shirkhoda A, Sokhandon F. Getting the GIST: a pictorial review of the various patterns of presentation of gastrointestinal stromal tumors on imaging. *Abdom Radiol (NY)* 2017; 1350-1364 [DOI: 10.1007/s00261-016-1025-z]
3 **Joensuu H**, Hohenberger P, Corless CL. Gastrointestinal stromal tumour. *Lancet* 2013; **382**: 973-983 [PMID: 23623056 DOI: 10.1016/S0140-6736(13)60106-3]
4 **von Mehren M**, Joensuu H. Gastrointestinal Stromal Tumors. *J Clin Oncol* 2018; **36**: 136-143 [PMID: 29220298 DOI: 10.1200/JCO.2017.74.9705]
5 **Joensuu H**. Risk stratification of patients diagnosed with gastrointestinal stromal tumor. *Hum Pathol* 2008; **39**: 1411-1419 [PMID: 18774375 DOI: 10.1016/j.humpath.2008.06.025]
6 **Miettinen M**, Lasota J. Gastrointestinal stromal tumors: pathology and prognosis at different sites. *Semin Diagn Pathol* 2006; **23**: 70-83 [PMID: 17193820 DOI: 10.1053/j.semdp.2006.09.001]
7 **Wang Y**, Wang Y, Ren J, Jia L, Ma L, Yin X, Yang F, Gao BL. Malignancy risk of gastrointestinal stromal tumors evaluated with noninvasive radiomics: A multi-center study. *Front Oncol* 2022; **12**: 966743 [PMID: 36052224 DOI: 10.3389/fonc.2022.966743]
8 **Theiss L**, Contreras CM. Gastrointestinal Stromal Tumors of the Stomach and Esophagus. *Surg Clin North Am* 2019; **99**: 543-553 [PMID: 31047041 DOI: 10.1016/j.suc.2019.02.012]
9 **Ma X**, Ling W, Xia F, Zhang Y, Zhu C, He J. Application of Contrast-Enhanced Ultrasound (CEUS) in Lymphomatous Lymph Nodes: A Comparison between PET/CT and Contrast-Enhanced CT. *Contrast Media Mol Imaging* 2019; **2019**: 5709698 [PMID: 30809108 DOI: 10.1155/2019/5709698]
10 **Li C**, Fu W, Huang L, Chen Y, Xiang P, Guan J, Sun C. A CT-based nomogram for predicting the malignant potential of primary gastric gastrointestinal stromal tumors preoperatively. *Abdom Radiol (NY)* 2021; **46**: 3075-3085 [PMID: 33713161 DOI: 10.1007/s00261-021-03026-7]
11 **Danti G**, Addeo G, Cozzi D, Maggialetti N, Lanzetta MM, Frezzetti G, Masserelli A, Pradella S, Giovagnoni A, Miele V. Relationship between diagnostic imaging features and prognostic outcomes in gastrointestinal stromal tumors (GIST). *Acta Biomed* 2019; **90**: 9-19 [PMID: 31085970 DOI: 10.23750/abm.v90i5-S.8343]
12 **Zhou C**, Duan X, Zhang X, Hu H, Wang D, Shen J. Predictive features of CT for risk stratifications in patients with primary gastrointestinal stromal tumour. *Eur Radiol* 2016; **26**: 3086-3093 [PMID: 26699371 DOI: 10.1007/s00330-015-4172-7]
13 **Li H**, Ren G, Cai R, Chen J, Wu X, Zhao J. A correlation research of Ki67 index, CT features, and risk stratification in gastrointestinal stromal tumor. *Cancer Med* 2018; **7**: 4467-4474 [PMID: 30123969 DOI: 10.1002/cam4.1737]
14 **Tang B**, Feng QX, Liu XS. Comparison of Computed Tomography Features of Gastric and Small Bowel Gastrointestinal Stromal Tumors With Different Risk Grades. *J Comput Assist Tomogr* 2022; **46**: 175-182 [PMID: 35297574 DOI: 10.1097/RCT.0000000000001262]
15 **Kim JS**, Kim HJ, Park SH, Lee JS, Kim AY, Ha HK. Computed tomography features and predictive findings of ruptured gastrointestinal stromal tumours. *Eur Radiol* 2017; **27**: 2583-2590 [PMID: 27761711 DOI: 10.1007/s00330-016-4515-z]
16 **Maldonado FJ**, Sheedy SP, Iyer VR, Hansel SL, Bruining DH, McCollough CH, Harmsen WS, Barlow JM, Fletcher JG. Reproducible imaging features of biologically aggressive gastrointestinal stromal tumors of the small bowel. *Abdom Radiol (NY)* 2018; **43**: 1567-1574 [PMID: 29110055 DOI: 10.1007/s00261-017-1370-6]
17 **Inoue A**, Ota S, Nitta N, Murata K, Shimizu T, Sonoda H, Tani M, Ban H, Inatomi O, Ando A, Kushima R, Watanabe Y. Difference of computed tomographic characteristic findings between gastric and intestinal gastrointestinal stromal tumors. *Jpn J Radiol* 2020; **38**: 771-781 [PMID: 32246352 DOI: 10.1007/s11604-020-00962-0]
18 **Zhang X**, Bai L, Wang D, Huang X, Wei J, Zhang W, Zhang Z, Zhou J. Gastrointestinal stromal tumor risk classification: spectral CT quantitative parameters. *Abdom Radiol (NY)* 2019; **44**: 2329-2336 [PMID: 30980116 DOI: 10.1007/s00261-019-01973-w]
19 **Mazzei MA**, Cioffi Squitieri N, Vindigni C, Guerrini S, Gentili F, Sadotti G, Mercuri P, Righi L, Lucii G, Mazzei FG, Marrelli D, Volterrani L. Gastrointestinal stromal tumors (GIST): a proposal of a "CT-based predictive model of Miettinen index" in predicting the risk of malignancy. *Abdom Radiol (NY)* 2020; **45**: 2989-2996 [PMID: 31506758 DOI: 10.1007/s00261-019-02209-7]
20 **Su Q**, Wang Q, Zhang H, Yu D, Wang Y, Liu Z, Zhang X. Computed tomography findings of small bowel gastrointestinal stromal tumors with different histologic risks of progression. *Abdom Radiol (NY)* 2018; **43**: 2651-2658 [PMID: 29492604 DOI: 10.1007/s00261-018-1511-6]
21 **Chen Z**, Yang J, Sun J, Wang P. Gastric gastrointestinal stromal tumours (2-5 cm): Correlation of CT features with malignancy and differential diagnosis. *Eur J Radiol* 2020; **123**: 108783 [PMID: 31841880 DOI: 10.1016/j.ejrad.2019.108783]
22 **Peng G**, Huang B, Yang X, Pang M, Li N. Preoperative CT feature of incomplete overlying enhancing mucosa as a high-risk predictor in gastrointestinal stromal tumors of the stomach. *Eur Radiol* 2021; **31**: 3276-3285 [PMID: 33125563 DOI: 10.1007/s00330-020-07377-5]
23 **Rubin BP**, Heinrich MC, Corless CL. Gastrointestinal stromal tumour. *Lancet* 2007; **369**: 1731-1741 [PMID: 17512858 DOI: 10.1016/S0140-6736(07)60780-6]
24 **Xu D**, Si GY, He QZ. Correlation analysis of multi-slice computed tomography (MSCT) findings, clinicopathological factors, and prognosis of gastric gastrointestinal stromal tumors. *Transl Cancer Res* 2020; **9**: 1787-1794 [PMID: 35117526 DOI: 10.21037/tcr.2020.02.26]
25 **Cho JW**; Korean ESD Study Group. Current Guidelines in the Management of Upper Gastrointestinal Subepithelial Tumors. *Clin Endosc* 2016; **49**: 235-240 [PMID: 26898512 DOI: 10.5946/ce.2015.096]
26 **Iannicelli E**, Carbonetti F, Federici GF, Martini I, Caterino S, Pilozzi E, Panzuto F, Briani C, David V. Evaluation of the Relationships Between Computed Tomography Features, Pathological Findings, and Prognostic Risk Assessment in Gastrointestinal Stromal Tumors. *J Comput Assist Tomogr* 2017; **41**: 271-278 [PMID: 27753723 DOI: 10.1097/RCT.0000000000000499]

27 **Wang M**, Feng Z, Zhou L, Zhang L, Hao X, Zhai J. Computed-Tomography-Based Radiomics Model for Predicting the Malignant Potential of Gastrointestinal Stromal Tumors Preoperatively: A Multi-Classifier and Multicenter Study. *Front Oncol* 2021; **11**: 582847 [PMID: 33968714 DOI: 10.3389/fonc.2021.582847]

28 **Chen T**, Xu L, Dong X, Li Y, Yu J, Xiong W, Li G. The roles of CT and EUS in the preoperative evaluation of gastric gastrointestinal stromal tumors larger than 2 cm. *Eur Radiol* 2019; **29**: 2481-2489 [PMID: 30617491 DOI: 10.1007/s00330-018-5945-6]

29 **Wei SC**, Xu L, Li WH, Li Y, Guo SF, Sun XR, Li WW. Risk stratification in GIST: shape quantification with CT is a predictive factor. *Eur Radiol* 2020; **30**: 1856-1865 [PMID: 31900704 DOI: 10.1007/s00330-019-06561-6]

30 **Liu X**, Qiu H, Zhang P, Feng X, Chen T, Li Y, Tao K, Li G, Sun X, Zhou Z; China Gastrointestinal Stromal Tumor Study Group (CN-GIST). Prognostic role of tumor necrosis in patients undergoing curative resection for gastric gastrointestinal stromal tumor: a multicenter analysis of 740 cases in China. *Cancer Med* 2017; **6**: 2796-2803 [PMID: 29058376 DOI: 10.1002/cam4.1229]

31 **Yang HK**, Kim YH, Lee YJ, Park JH, Kim JY, Lee KH, Lee HS. Leiomyomas in the gastric cardia: CT findings and differentiation from gastrointestinal stromal tumors. *Eur J Radiol* 2015; **84**: 1694-1700 [PMID: 26051977 DOI: 10.1016/j.ejrad.2015.05.022]

32 **Hong X**, Choi H, Loyer EM, Benjamin RS, Trent JC, Charnsangavej C. Gastrointestinal stromal tumor: role of CT in diagnosis and in response evaluation and surveillance after treatment with imatinib. *Radiographics* 2006; **26**: 481-495 [PMID: 16549611 DOI: 10.1148/rg.262055097]

Published by **Baishideng Publishing Group Inc**
7041 Koll Center Parkway, Suite 160, Pleasanton, CA 94566, USA
Telephone: +1-925-3991568
E-mail: bpgoffice@wjgnet.com
Help Desk: https://www.f6publishing.com/helpdesk
https://www.wjgnet.com